AMERICAN SOCIETY FOR MICROBIOLOGY | Antimicrobial Agents and Chemotherapy

Stringent Response Factors PPX1 and PPK2 Play an Important Role in *Mycobacterium tuberculosis* Metabolism, Biofilm Formation, and Sensitivity to Isoniazid *In Vivo*

Yu-Min Chuang,[a] Noton K. Dutta,[b] Chien-Fu Hung,[a,c] T.-C. Wu,[a,c,d,e] Harvey Rubin,[f] Petros C. Karakousis[b,g]

Department of Pathology, Johns Hopkins University School of Medicine, Baltimore, Maryland, USA[a]; Department of Medicine, Johns Hopkins University School of Medicine, Baltimore, Maryland, USA[b]; Department of Oncology, Johns Hopkins University School of Medicine, Baltimore, Maryland, USA[c]; Department of Obstetrics and Gynecology, Johns Hopkins University School of Medicine, Baltimore, Maryland, USA[d]; Department of Molecular Microbiology and Immunology, Johns Hopkins University School of Medicine, Baltimore, Maryland, USA[e]; Department of Medicine, University of Pennsylvania Perelman School of Medicine, Philadelphia, Pennsylvania, USA[f]; Department of International Health, Johns Hopkins Bloomberg School of Public Health, Baltimore, Maryland, USA[g]

***Mycobacterium tuberculosis* remains a global health threat largely due to the lengthy duration of curative antibiotic treatment, contributing to medical nonadherence and the emergence of drug resistance. This prolonged therapy is likely due to the presence of *M. tuberculosis* persisters, which exhibit antibiotic tolerance. Inorganic polyphosphate [poly(P)] is a key regulatory molecule in the *M. tuberculosis* stringent response mediating antibiotic tolerance. The polyphosphate kinase PPK1 is responsible for poly(P) synthesis in *M. tuberculosis*, while the exopolyphosphatases PPX1 and PPX2 and the GTP synthase PPK2 are responsible for poly(P) hydrolysis. In the present study, we show by liquid chromatography-tandem mass spectrometry that poly(P)-accumulating *M. tuberculosis* mutant strains deficient in *ppx1* or *ppk2* had significantly lower intracellular levels of glycerol-3-phosphate (G3P) and 1-deoxy-xylulose-5-phosphate. Real-time PCR revealed decreased expression of genes in the G3P synthesis pathway in each mutant. The *ppx1*-deficient mutant also showed a significant accumulation of metabolites in the tricarboxylic acid cycle, as well as altered arginine and NADH metabolism. Each poly(P)-accumulating strain showed defective biofilm formation, while deficiency of *ppk2* was associated with increased sensitivity to plumbagin and meropenem and deficiency of *ppx1* led to enhanced susceptibility to clofazimine. A DNA vaccine expressing *ppx1* and *ppk2*, together with two other members of the *M. tuberculosis* stringent response, *M. tuberculosis rel* and *sigE*, did not show protective activity against aerosol challenge with *M. tuberculosis*, but vaccine-induced immunity enhanced the killing activity of isoniazid in a murine model of chronic tuberculosis. In summary, poly(P)-regulating factors of the *M. tuberculosis* stringent response play an important role in *M. tuberculosis* metabolism, biofilm formation, and antibiotic sensitivity *in vivo*.**

Mycobacterium tuberculosis remains a major threat to global public health (1). The primary obstacles to eradication of *M. tuberculosis* infection are the need for combination antibiotic treatment and the prolonged duration of treatment, which is believed to be due to the presence of replication-deficient, antibiotic-tolerant persistent bacteria or persisters (2). An improved understanding of the regulatory pathways underlying persister formation is paramount to the development of novel strategies to more effectively target these persisters, thereby shortening the duration of tuberculosis (TB) treatment.

The stringent response (SR) regulatory molecules inorganic polyphosphate [poly(P)] and hyperphosphorylated guanosine [(p)ppGpp] have been shown to mediate persister formation in bacteria (3–5). Although the mechanism remains unclear, (p)ppGpp induces toxin-antitoxin systems, leading to increased numbers of persisters in *Escherichia coli* (5, 6). *M. tuberculosis* expresses two polyphosphate kinases (PPK1, PPK2) and two exopolyphosphatases (PPX1, PPX2) to regulate intracellular poly(P) homeostasis (7–10). PPK1 synthesizes poly(P) through hydrolysis of ATP (4). Although PPK2 enzymes can synthesize poly(P), *M. tuberculosis* PPK2 has nucleoside diphosphate kinase A-like activity (11), catalyzing poly(P) hydrolysis and ATP synthesis 800-fold faster than poly(P) synthesis (12). The mycobacterial stringent response appears to be a positive-feedback loop, as poly(P) phosphorylates and activates the two-component system MprAB, which induces expression of *sigE* and *M. tuberculosis rel* (rel_{Mtb}) (13), leading to increased synthesis of (p)ppGpp, which inhibits the hydrolysis of poly(P) by PPX2 (10). Poly(P) accumulation is associated with antibiotic tolerance (9–11), and poly(P) deficiency renders *M. tuberculosis* more sensitive to antibiotics (14). In addition, poly(P) homeostasis is required for *M. tuberculosis* survival during acute infection in murine lungs (15) and during chronic infection in guinea pig lungs (11, 14). Previously, we found that an *M. tuberculosis ppx2* (*Rv1026*) knockdown strain showed global transcriptional changes, including reduced expression of genes encoding enzymes involved in glycerol-3-phosphate (G3P) synthesis (10). This recombinant strain also displayed altered cell wall thickness and permeability and tolerance to the cell wall-active

Received 27 May 2016 **Returned for modification** 17 June 2016
Accepted 9 August 2016

Accepted manuscript posted online 15 August 2016

Citation Chuang Y-M, Dutta NK, Hung C-F, Wu T-C, Rubin H, Karakousis PC. 2016. Stringent response factors PPX1 and PPK2 play an important role in *Mycobacterium tuberculosis* metabolism, biofilm formation, and sensitivity to isoniazid *in vivo*. Antimicrob Agents Chemother 60:6460–6470. doi:10.1128/AAC.01139-16.

Address correspondence to Petros C. Karakousis, petros@jhmi.edu.

Supplemental material for this article may be found at http://dx.doi.org/10.1128/AAC.01139-16.

Copyright © 2016, American Society for Microbiology. All Rights Reserved.

agent isoniazid. However, it is unknown whether these profound metabolic and phenotypic changes were a specific consequence of *ppx2* deficiency or were more generally related to poly(P) accumulation.

In the current study, we studied the metabolome and gene expression of two poly(P)-accumulating strains containing transposon insertions in the *ppx1* (*MT0516*) gene or the *ppk2* gene (the *ppx1*::Tn and *ppk2*::Tn mutants, respectively) (9, 15). In addition, we determined the susceptibility of each strain to various antibiotics and other stresses, as well as their ability to develop biofilms, a potentially important property of persistent *M. tuberculosis* infection (16, 17). Finally, in order to investigate the role of the *M. tuberculosis* stringent response pathway in bacillary persistence during antibiotic treatment of chronic murine *M. tuberculosis* infection, we evaluated the therapeutic efficacy of an adjuvant DNA vaccine expressing *ppx1*, *ppk2*, as well as *sigE* and rel_{Mtb}, two other members of the positive-feedback cascade regulating *M. tuberculosis* intracellular poly(P) homeostasis. Our results suggest that enhanced immunity targeting the *M. tuberculosis* stringent response pathway promotes host control of mycobacteria during antibiotic treatment in mice.

MATERIALS AND METHODS

Bacteria and growth conditions. Wild-type *M. tuberculosis* CDC1551 strains deficient in *ppx1* (*MT0516*) (the *ppx1*::Tn mutant) and *ppk2* (*Rv3232c*) (the *ppk2*::Tn mutant) were generated by transposon mutagenesis, and the respective complemented strains, the *ppx1*::Tn Comp and *ppk2*::Tn Comp strains, were generated and genetically and phenotypically confirmed as previously described (9, 15). All strains, including wild-type strain *M. tuberculosis* CDC1551, were grown in Middlebrook 7H9 broth (Difco, Sparks, MD) supplemented with 10% oleic acid-albumin-dextrose-catalase (OADC; Difco), 0.1% glycerol, and 0.05% Tween 80 at 37°C on a roller.

Metabolomics analysis. Sample preparation and analysis were performed as previously described (10, 18). Briefly, mid-logarithmically growing cultures (optical density [OD] = 0.5) of the *ppx1*::Tn, *ppk2*::Tn, and wild-type strains were pelleted, and the samples were extracted in 1 ml of extraction buffer (chloroform-methanol, 2:1) and then concentrated by centrifugal evaporation. The samples were processed and analyzed by ultra-high-performance liquid chromatography-tandem mass spectrometry (UHPLC/MS/MS) and gas chromatography-mass spectrometry (GC/MS) by Metabolon, Inc. (Durham, NC) (19, 20). Statistical analysis of log-transformed data was performed (10), and Welch's *t* tests were performed to compare data between experimental groups. Multiple comparisons were accounted for by estimating the false discovery rate (FDR) using *q* values (21).

Sensitivity to plumbagin, meropenem, and clofazimine by disk diffusion. Each *M. tuberculosis* strain was grown in enriched 7H9 broth until mid-log growth phase, and 10^7 bacteria were plated on Middlebrook 7H10 plates. Plumbagin (10 μl of 20 mM or 100 mM dissolved in ethanol), meropenem (10 μg/ml or 20 μg/ml dissolved in water), or clofazimine (10 μg/ml dissolved in dimethyl sulfoxide) was added to separate sterile disks, which were placed on plates individually. The zone of growth inhibition was measured after 10 days of incubation, and each drug concentration was tested for each strain in triplicate (22).

Biofilm formation assay and crystal violet staining. Crystal violet staining was performed as described previously (23) with minor modifications. Briefly, mid-log-phase cultures (0.5 ml; density, 10^6 cells/ml) were grown in 24-well conical-bottom plates in Sauton's medium without detergent and shaking for 5 weeks. The extracellular matrix of the biofilm was measured by crystal violet staining using a FLUOstar Optima reader (BMG Labtech).

RT-PCR. Real-time PCR (RT-PCR) was performed as previously described (15). The gene-specific primers used are listed in Table S2 in the supplemental material.

Ethidium bromide accumulation/efflux assay and Nile red uptake assays. The results of the ethidium bromide accumulation and efflux assays were determined by measurement of the florescence intensity (10). For Nile red uptake staining, mid-log-phase cultures were washed with phosphate-buffered saline (PBS) and then stained with 20 μM Nile red (Sigma) (24). In all assays, the cells were incubated in 96-well plates, and analysis was performed at the time points indicated below by the use of excitation at 544 nm and emission at 590 nm with a FLUOstar Optima reader (BMG Labtech). All data were normalized to the reading of each well at time zero.

Antigen preparation. The open reading frames of the *ppx1*, *ppk2*, and *sigE* genes were amplified from *M. tuberculosis* CDC1551 and cloned individually into plasmid pET28a using the restriction enzymes NdeI and BamHI (see Table S3 in the supplemental material). A previously generated plasmid expressing rel_{Mtb}, pET15b[rel_{Mtb}] (25), was used for expression of the Rel_{Mtb} protein. The resulting plasmids were used to transform *E. coli* BL21(DE3) RP competent cells (Stratagene). The transformed bacteria were selected by kanamycin (50 μg/ml) or ampicillin (100 μg/ml), and cloning was confirmed by DNA sequencing. The expression and purification of the protein were performed using standard protocols (Qiagen).

DNA vaccination of mice. The plasmid pSectag2B was used to express individual genes, *ppx1*, *ppk2*, rel_{Mtb}, and *sigE*. Briefly, each gene was cloned individually into pSectag2B using the restriction enzymes BamHI and HindIII (see Table S3 in the supplemental material). The insertion was confirmed by sequencing, and the expression of target genes was confirmed by transfection of 293T cells. Each DNA vaccine was delivered as previously described (26, 27), and all procedures were performed according to protocols approved by the Johns Hopkins University Institutional Animal Care and Use Committee. Briefly, each plasmid was delivered by intramuscular injection into the quadriceps femoris muscle of the mice, followed by local electroporation using an ECM830 square wave electroporation system (BTX Harvard Apparatus Company, Holliston, MA, USA). Each of the two-needle array electrodes delivered 15 pulses of 72 V (a 20-ms pulse duration at 200-ms intervals). Ten micrograms of each plasmid was injected into each hind leg once weekly for 3 weeks. One week after the last vaccination, the mice were scarified and the blood and splenocytes were collected (27).

ELISA. Antigen-specific antibody responses were measured by enzyme-linked immunoabsorbent assay (ELISA) as described previously (28), with minor modifications in the coating and serum incubation steps. The 96-well microplate was coated with 1 μg/ml of purified Rel_{Mtb} or SigE protein overnight. For PPK2 or PPX1, the coating concentration was 5 μg/ml. After blocking, sera from vaccinated mice were diluted 1:100 with PBS, and the diluted sera were added to wells and incubated at room temperature for 2 h.

Intracellular cytokine staining and flow cytometry analysis. To detect antigen-specific $CD4^+$ T-cell responses by intracellular staining for gamma interferon (IFN-γ), splenocytes were stimulated individually with one of the purified recombinant proteins, PPK2, PPX1, Rel_{Mtb}, or SigE (10 μg/ml), for 24 h at 37°C before addition of GolgiPlug cocktail (BD Pharmingen, San Diego, CA) overnight. After incubation, the splenocytes were washed once with FACScan buffer and then stained with phycoerythrin-conjugated monoclonal rat anti-mouse CD4. The cells were permeabilized using a Cytofix/Cytoperm kit (BD Pharmingen, San Diego, CA). Intracellular IFN-γ was stained with fluorescein isothiocyanate-conjugated rat anti-mouse IFN-γ and allophycocyanin-conjugated rat anti-mouse tumor necrosis factor alpha (TNF-α; BD Pharmingen, San Diego, CA). Flow cytometry was performed with a FACSCalibur flow cytometer, and the results were analyzed with FlowJo software.

Aerosol infection of mice with *M. tuberculosis* and DNA vaccine study endpoints. The stringent response (SR) vaccine, containing 5 μg of each plasmid expressing *ppx1*, *ppk2*, rel_{Mtb}, or *sigE* was delivered as described above once weekly for 4 weeks. The empty vector, pSectag2B (20 μg), was given as sham vaccine. At 3 weeks after the last vaccine dose, mice were aerosol infected with ~100 bacilli of wild-type *M. tuberculosis* CDC1551. Mice were sacrificed on days 14 and 56 after aerosol challenge, and the lungs were homogenized and plated for determination of the number of CFU (15) to evaluate the protective efficacy of the SR vaccine. Separate groups of naive, vaccinated, and sham-vaccinated mice were treated with isoniazid (10 mg/kg of body weight) by esophageal gavage once daily (5 days/week) for 4 weeks beginning on day 14 after aerosol challenge. The lungs were homogenized and plated after 56 days of isoniazid treatment to determine the number of CFU. A partial sample of each infected lung was fixed with 10% buffered formaldehyde, processed, and paraffin embedded for histological staining with hematoxylin and eosin. Morphometric analysis of histology sections was performed as previously described (29).

Statistical analysis. Data from at least three biological replicates were used to calculate means and standard deviations (SDs) for graphing purposes. Statistical analysis employed the unpaired Student's *t* test, and a *P* value of <0.05 was considered statistically significant.

RESULTS

Polyphosphate accumulation alters the metabolic profile of *M. tuberculosis*. Previously, we have shown that *M. tuberculosis* mutant strains deficient in *ppk2* or *ppx1* accumulate poly(P) relative to the level of poly(P) accumulated by the isogenic wild-type strain (9, 15). The *ppx1* mutant showed higher levels of expression of the rel_{Mtb}, *sigE*, and *mprB* genes by RT-PCR during mid-log-phase growth (9), while the *ppk2*-deficient mutant showed a higher level of expression of *sigE* (change in the threshold cycle value [ΔC_T] = 1.26; $P = 0.035$) but a lower level of expression of *mprB* ($-\Delta C_T = -0.75$; $P = 0.017$) and unchanged expression of rel_{Mtb} ($-\Delta C_T = -0.25$; $P = 0.4$) compared to the level of expression by the isogenic wild-type strain during late-log phase growth after normalization to the level of *sigA* expression. We used metabolomics to further characterize the physiological changes in these two poly(P)-accumulating mutants (see Table S1 in the supplemental material). In addition to the accumulation of poly(P) and pyrophosphate, both strains had significantly lower levels of glycerol-3-phosphate (G3P) and glycerol-2-phosphate (G2P) (Fig. 1A). The peptidoglycan biosynthetic metabolite 1-deoxy-xylulose-5-phosphate (DXP), which is required for the synthesis of isoprenoid (30), was also less abundant in the mutant strains (Fig. 1B). These changes suggest that peptidoglycan synthesis may be affected by poly(P) accumulation. NAD is a cofactor utilized in several redox reactions that are vital to metabolism. The levels of the oxidized form of the metabolite NAD^+ were increased in the *ppx1*::Tn mutant relative to those in wild-type bacilli (Fig. 1C). The level of nicotinate ribonucleoside, an intermediate in the salvage pathway of NAD, was significantly reduced in both the *ppk2*::Tn and *ppx1*::Tn mutants. The level of nicotinic acid mononucleotide (NaMN), an intermediate in the *de novo* synthesis pathway of NAD, was relatively lower in both strains. These findings suggest that the intracellular NAD pool may be regenerated by salvage pathways in these mutant bacteria.

Lipid oxidation and citrate cycle activity increase during polyphosphate accumulation in the *ppk2* and *ppx1* mutant strains. The *ppx1*::Tn strain showed an increased abundance of several metabolites indicative of increased lipid oxidation, including acetyl coenzyme A (CoA), propionyl-CoA, and 2-methylcitrate (see Table S1 in the supplemental material). Acetyl-CoA can be formed from the oxidation of even-numbered-chain fatty acids, and propionyl-CoA is often generated from the oxidation of odd-numbered-chain fatty acids. Both acetyl-CoA and propionyl-CoA can enter the citric acid cycle to produce precursors for amino acids, lipids, and energy. When propionyl-CoA enters the citric acid cycle, the metabolite 2-methylcitrate is generated. In addition to acetyl-CoA and 2-methylcitrate, the levels of several other citric acid cycle intermediates were elevated in the *ppx1*::Tn strain, including malate and succinate (Fig. 1D). An increase in the amounts of citric acid cycle intermediates was also observed in the *ppk2*::Tn mutant, possibly reflecting a need to generate larger amounts of metabolites involved in energy production, such as NADH.

Several amino acid metabolites were more abundant in the poly(P)-accumulating strains, especially in the *ppx1*::Tn mutant (see Table S1 in the supplemental material). The arginine deiminase pathway provides a mechanism by which ATP can be generated from the metabolism of arginine. In this pathway, arginine is converted to citrulline, which is then converted to ornithine and carbamoyl phosphate. ATP can be generated when carbamoyl phosphate is dephosphorylated by carbamate kinase (31, 32). This pathway is known to be particularly active in response to environmental stress (33, 34) and is of special interest since poly(P) accumulation is associated with bacterial stress resistance. The levels of arginine, citrulline, and ornithine were higher in the *ppk2*::Tn and *ppx1*::Tn mutants than in the wild type (Fig. 1E). The increase in the amounts of the intermediates of this pathway may reflect an increased demand for energy and could serve as a potential mechanism by which these strains resist different stresses.

***M. tuberculosis* polyphosphate accumulation is associated with altered expression of G3P-related genes.** On the basis of the findings presented in our previous report (10) and those from the current study, *M. tuberculosis* poly(P) accumulation is associated with significantly decreased levels of G3P. This may be due to either decreased *de novo* synthesis of G3P or increased turnover. Several *M. tuberculosis* genes encode enzymes that regulate G3P homeostasis (35). Using RT-PCR, we analyzed the expression levels of these genes in the *ppk2* and *ppx1* mutant strains (Fig. 2). The genes encoding proteins responsible for G3P synthesis from dihydroxyacetone phosphate (*Rv0564c*) or hydrolysis (*glpD1*, *glpD2*) were significantly downregulated in the *ppx1*::Tn mutant compared to their level of regulation in the wild type. Among the genes involved in recycling of the glycerophospholipid polar head, *Rv2182c* was significantly downregulated in both mutant strains. The gene encoding the enzyme responsible for the synthesis of G3P from glycerol (*glpK*) was downregulated in the *ppx1*::Tn mutant, while the gene encoding the enzyme responsible for G3P hydrolysis was upregulated in the *ppk2*::Tn mutant. Thus, poly(P) accumulation associated with a deficiency of *ppk2* or *ppx1* led to altered expression of genes involved in G3P homeostasis, contributing to a reduced intracellular G3P content.

Poly(P) homeostasis is required for *M. tuberculosis* biofilm formation. We found that biofilm formation was impaired in a poly(P)-accumulating strain deficient in the exopolyphosphatase *ppx2* gene (10). However, it is unclear if poly(P) homeostasis is generally required for biofilm formation or if this phenomenon was related specifically to PPX2 deficiency. The *ppx1*::Tn and *ppk2*::Tn mutants and their respective complemented strains were

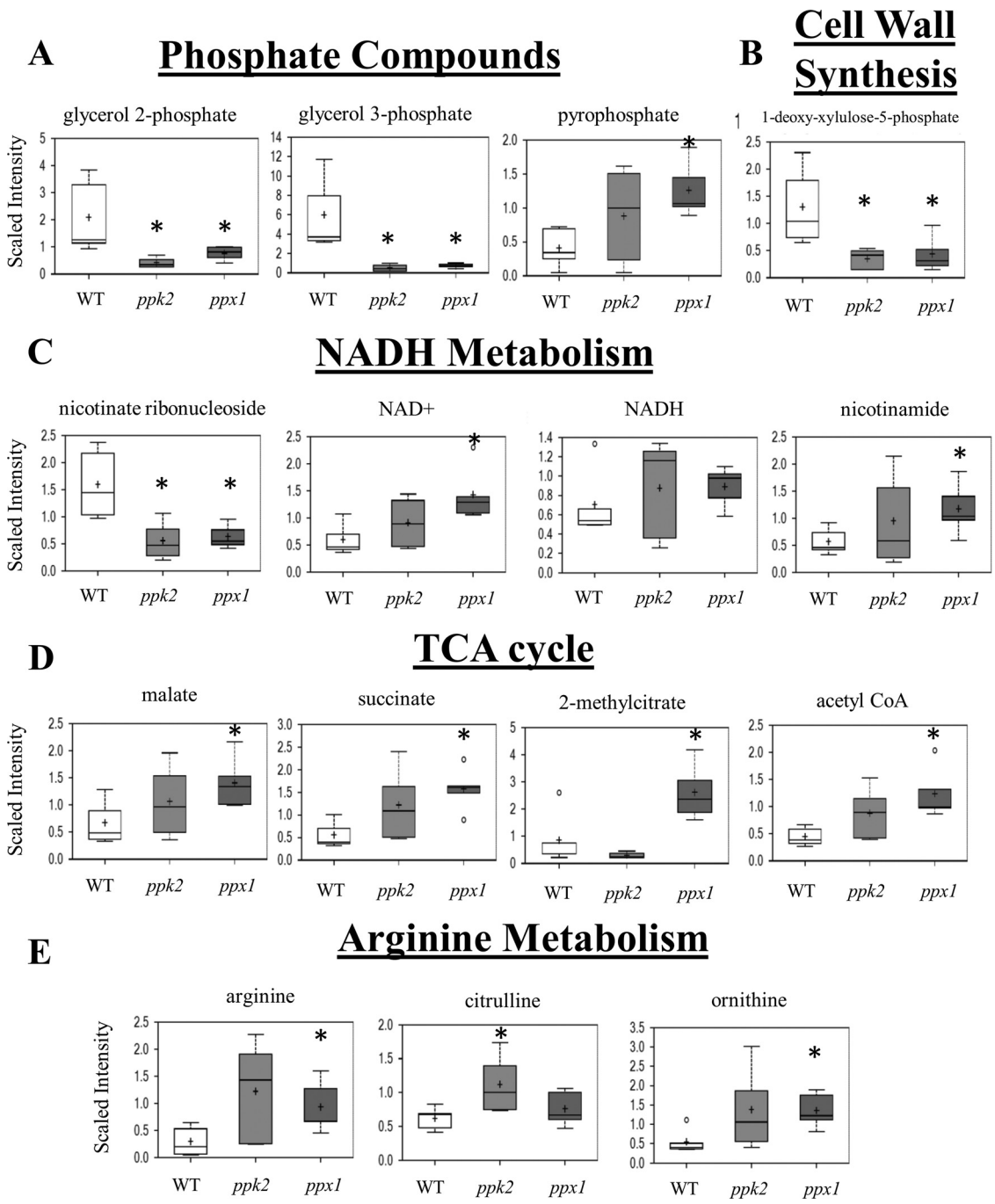

FIG 1 Polyphosphate accumulation alters *M. tuberculosis* metabolism. Metabolites altered in the *M. tuberculosis ppk2*-deficient and *ppx1*-deficient mutants relative to the wild-type strain include those belonging to the following categories: phosphate compounds (A), cell wall synthesis pathways (B), NADH metabolism (C), the citric acid (TCA) cycle (D), and arginine metabolism (E). WT, wild-type strain; *ppk2*, *ppk2*::Tn mutant; *ppx1*, *ppx1*::Tn mutant. The data represent 5 independent samples. *, $P < 0.05$ compared to the wild type.

grown in Sauton's medium for 5 to 6 weeks. As shown in Fig. 3, neither of the two mutant strains formed pellicle biofilms at the air-fluid interface. The pellicle formed by the *ppk2*::Tn complemented strain was less dense than that formed by the wild type, and the density of the pellicle formed by the *ppx1*::Tn complemented strain was similar to that of the pellicle formed by the wild type. Crystal violet staining corroborated the finding that *M. tuberculosis* poly(P) accumulation is associated with defective biofilm formation. It is unlikely that these results can be explained by defective growth in the mutants, since these differences persisted even after prolonged observation of cultures until the 8th week (data not shown).

Deficiency of *ppk2* leads to increased sensitivity to plumbagin and meropenem, while *ppx1* deficiency increases sensitivity to clofazimine. Previous studies have shown that meropenem inhibits both the D,D-carboxypeptidase and L,D-transpeptidase of

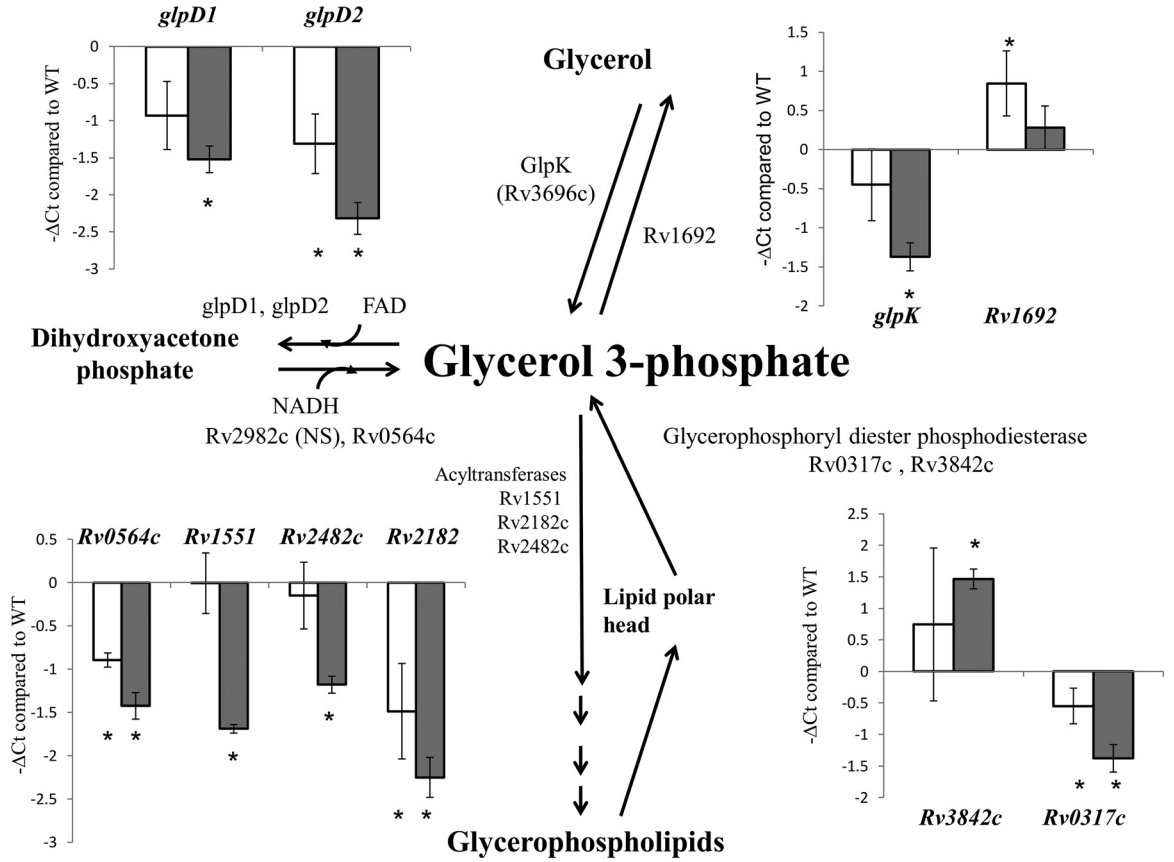

FIG 2 RT-PCR of *M. tuberculosis* genes related to glycerol-3-phosphate (G3P) metabolism during poly(P) accumulation. The C_T of each gene was normalized to that of the housekeeping gene *sigA* in each strain, and this value was subtracted from the similarly normalized C_T of each gene in the wild-type strain to yield the change in C_T (ΔC_T). Open bars, *ppk2*::Tn; gray bars, *ppx1*::Tn; error bars, SDs from at least three replicates; NS, no significant difference.

M. tuberculosis (36). L,D-Transpeptidase plays an important role in cell wall remodeling during mycobacterial entry into stationary phase (37). We studied the sensitivity of the *ppk2*::Tn and *ppx1*::Tn mutants to meropenem by the disk diffusion method (Table 1). The *ppk2*::Tn mutant showed increased sensitivity to meropenem at 10 μg/ml and 20 μg/ml, and the wild-type sensitivity pattern was partially restored in the *ppk2*::Tn complemented strain. Similarly, the *ppx1*::Tn mutant showed trends toward increased susceptibility to meropenem similar to those for the *ppk2*::Tn mutant, although this did not reach statistical significance. Next, we tested whether poly(P) accumulation altered mycobacterial resistance to oxidative stress (38). The *ppk2*::Tn mutant was more sensitive to the naphthoquinone plumbagin, and wild-type resistance was restored in the complemented strain. Similarly, the *ppx1*::Tn mutant showed mildly increased sensitivity to plumbagin compared to the wild type ($P = 0.1$). We then tested the effect of poly(P) accumulation on sensitivity to clofazimine, which destabilizes the bacterial membrane and alters redox cycling (39). Although *ppk2* deficiency did not alter clofazimine susceptibility, the *ppx1*::Tn mutant was more sensitive to clofazimine ($P = 0.006$), and wild-type levels of susceptibility were restored in the complemented strain.

Deficiency of *ppx1* or *ppk2* alters expression of peptidoglycan biosynthesis genes but does not alter cell wall permeability. The *ppk2*::Tn and *ppx1*::Tn mutants showed increased susceptibility to meropenem, suggesting potential changes in the mycobacterial cell wall structure associated with poly(P) accumulation. Our metabolomics analysis revealed a decreased abundance of 1-deoxy-D-xylulose-5-phosphate in both mutants. To investigate the possibility that poly(P) accumulation leads to altered peptidoglycan biosynthesis, we used RT-PCR to evaluate the expression of relevant genes (40). The genes encoding L,D-transpeptidase, *ldtA* and *ldtB*, were downregulated in both mutant strains (41). The *ppk2* mutant showed higher levels of expression of *pbpA*, while the *ppx1* mutant showed lower levels of expression than the wild type (Fig. 3C).

During macrophage infection, *M. tuberculosis* can acquire phenotypic tolerance to antibiotics through induction of efflux pumps (42). Previously, we found that a poly(P)-accumulating strain (*ppx2* knockdown) had altered cell wall permeability based on the results of an ethidium bromide uptake assay (10). In the current study, we did not observe any significant difference in ethidium bromide accumulation or efflux pump activity between each mutant and the respective complemented and wild-type strains (data not shown). For further evaluation of cell wall permeability, we used Nile red staining to determine whether deficiency of *ppx1* or *ppk2* was associated with altered rates of diffusion of lipophilic molecules across the *M. tuberculosis* cell wall (24). Nile red staining was equivalent between the *ppx1*::Tn mutant and the wild type, but the *ppk2*::Tn mutant showed reduced Nile red accumulation relative to the wild type (Fig. 4). The *ppk2* complemented strain showed uptake of Nile red similar to that of the wild type.

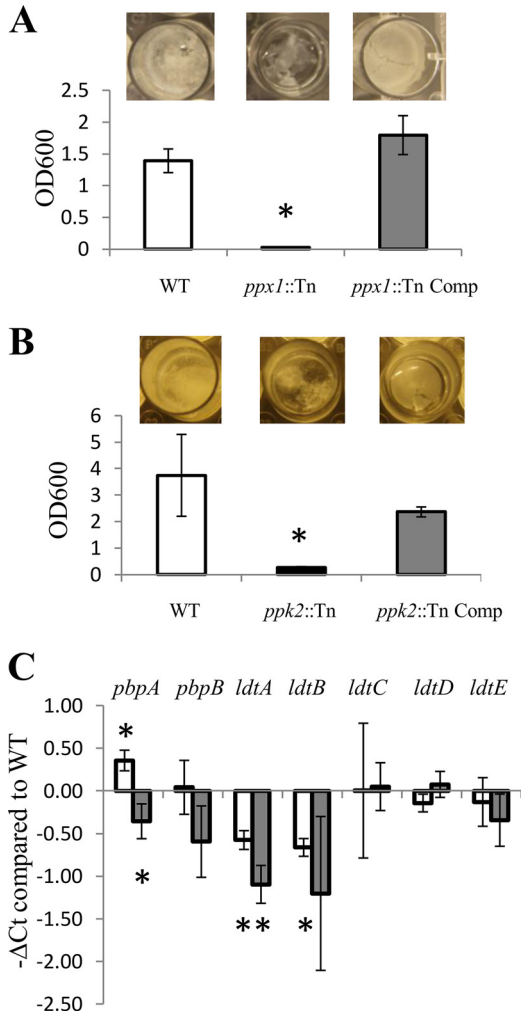

FIG 3 Polyphosphate accumulation alters expression of peptidoglycan biosynthesis genes and reduces biofilm formation. (A, B) The *ppx1*::Tn mutant (A) and the *ppk2*::Tn mutant (B) were incubated in Sauton's medium lacking detergent for 5 weeks, and biofilms were assessed by crystal violet staining (*, $P < 0.05$ relative to the wild type; $n = 3$). OD600, OD at 600 nm. (C) RT-PCR of *M. tuberculosis* genes related to peptidoglycan biosynthesis during mid-log phase of growth. The C_T of each gene was normalized to that of the housekeeping gene *sigA* in each strain, and this value was subtracted from the similarly normalized C_T of each gene in the wild-type strain to yield the change in C_T (ΔC_T). Open bars, *ppk2*::Tn mutant; gray bars, *ppx1*::Tn mutant; error bars, SDs. *, $P < 0.05$ relative to the wild type; $n = 3$.

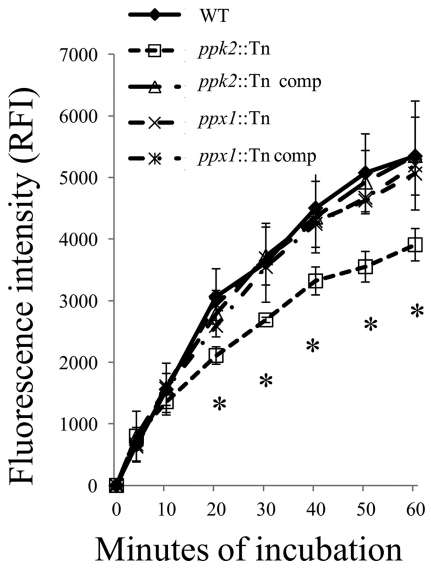

FIG 4 Decreased Nile red staining in the *ppk2*-deficient mutant. Each strain was grown to mid-log phase and stained with 20 μM Nile red. The fluorescence intensity was normalized to the initial signal. Data represent mean values ± SDs for three biological replicates. *, $P < 0.05$ when comparing *ppk2*::Tn mutants to the wild type or the *pp2*::Tn Comp strain. RFI, relative fluorescence intensity.

DNA vaccination with poly(P)-regulatory genes of the *M. tuberculosis* stringent response pathway generates antigen-specific CD4$^+$ T-cell responses and immunoglobulin. Although previous reports have highlighted the importance of poly(P)-regulatory genes in antibiotic tolerance and persistence in animal lungs (9, 15), it remains to be determined whether the stringent response pathway can be therapeutically targeted during chronic *M. tuberculosis* infection. To test this possibility, we first sought to determine whether specific immunity could be engendered to specific poly(P)-regulatory factors by DNA vaccination. We cloned four poly(P)-regulatory genes, rel_{Mtb}, *sigE*, *ppk2*, and *ppx*, individually into the eukaryotic expression plasmid pSectag2B. Separate groups of C57BL/6J mice were vaccinated intramuscularly with each of the plasmids carrying the individual genes or the empty vector once weekly for 3 weeks, and electroporation was performed immediately following each injection (Fig. 5A). Significant IgG responses to each antigen were detected by ELISA in the serum of vaccinated mice 1 week after the last DNA vaccine dose

TABLE 1 Sensitivity of each strain to plumbagin, meropenem, and clofazimine by the disk diffusion method

Drug (concn)	Inhibition zone diam (mm) for wild-type strain	*ppk2*::Tn mutant		*ppk2*::Tn Comp strain		*ppx1*::Tn mutant		*ppx1*::Tn Comp strain	
		Inhibition zone diam (mm)	*P* value	Inhibition zone diam (mm)	*P* value	Inhibition zone diam (mm)	*P* value	Inhibition zone diam (mm)	*P* value
Plumbagin									
20 mM	25 ± 1.7	32.7 ± 4.1	0.042	24.3 ± 0.6	0.561	25.7 ± 2.1	0.692	23.3 ± 0.6	0.189
100 mM	44 ± 1	49.3 ± 1.2	0.004	45.3 ± 4.2	0.618	47.3 ± 2.5	0.100	40.7 ± 2.3	0.083
Meropenem									
10 μg/ml	17.4 ± 1.2	24 ± 2	0.007	20.6 ± 1.2	0.024	19.4 ± 2.4	0.251	16 ± 0	0.116
20 μg/ml	26.6 ± 1.154	29.3 ± 1.2	0.047	31.3 ± 3.1	0.069	31.3 ± 3.2	0.077	32.6 ± 4.9	0.110
Clofazimine (10 μg/ml)	18.3 ± 0.57	18.6 ± 2.3	0.820	17.33 ± 1.2	0.251	21 ± 1	0.006	20.3 ± 1.2	0.055

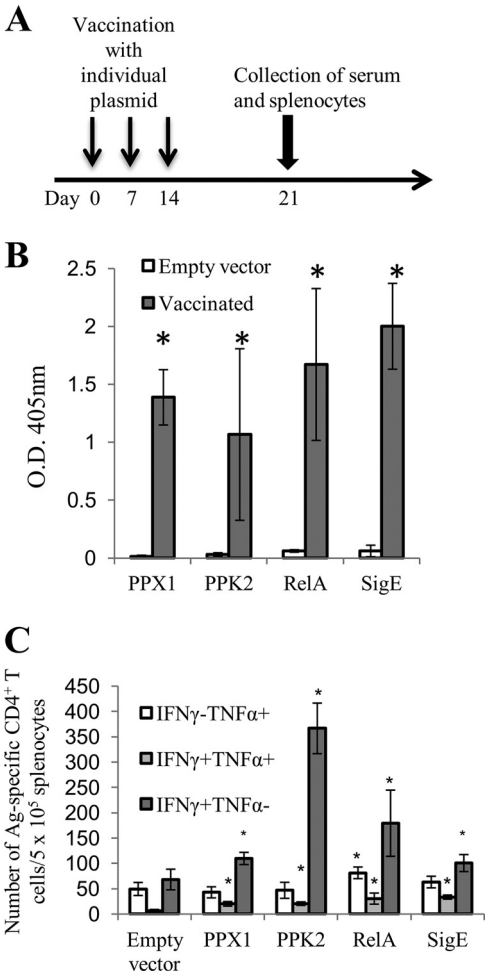

FIG 5 Immunogenicity of DNA vaccines targeting poly(P)-regulatory genes. (A) Six- to 8-week-old female C57BL/6J mice ($n = 3$ or 4) were vaccinated with DNA plasmid (pSectag2B) encoding rel_{Mtb}, *sigE*, *ppx1*, or *ppk2* or the empty vector, as illustrated in the scheme. Vaccination and electroporation were performed once weekly for 3 weeks. At 1 week after the last vaccination, sera and splenocytes were collected from each group. (B) ELISA detection of antigen-specific IgG responses from the different mouse vaccination groups. (C) Summary of antigen (Ag)-specific $CD4^+$ T-cell responses (positive intracellular staining for IFN-γ [IFN-γ^+] and TNF-α [TNF-α^+]) following DNA vaccination. Splenocytes from the individual vaccinated groups were stimulated with 10 μg/ml of each recombinant protein for 24 h at 37°C, and then GolgiPlug cocktail (1 μl/ml) was added overnight. The cells were then stained with anti-mouse CD4, followed by positive intracellular staining for IFN-γ and TNF-α. The data were acquired with a FACSCalibur flow cytometer and analyzed with FlowJo software. *, $P < 0.05$ compared to the empty vector control. IFN-γ^- and TNF-α^-, negative intracellular staining for IFN-γ and TNF-α, respectively.

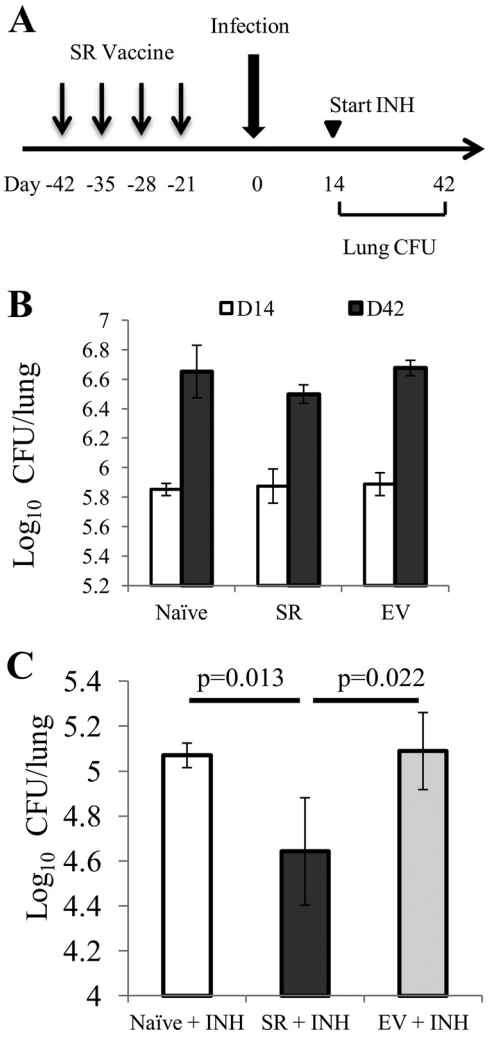

FIG 6 Immunity to key poly(P)-regulatory factors of the *M. tuberculosis* stringent response augments the bactericidal activity of isoniazid in mice. (A) Experimental scheme. C57BL/6J mice were vaccinated intramuscularly once weekly with the SR vaccine comprising four different DNA plasmids, each of which carried the rel_{Mtb}, *sigE*, *ppx1*, or *ppk2* gene, or with a sham vaccine (empty vector [EV]). A separate group of mice received no vaccination (naive). Three weeks later, all mice were aerosol infected with wild-type *M. tuberculosis*. Beginning on day 14 after aerosol infection, subgroups of mice in each group were treated orally with human-equivalent doses of isoniazid for 4 weeks. INH, isoniazid at 10 mg/kg by esophageal gavage once daily (5 days/week). (B) Lung bacillary burden ($\log_{10}$ number of CFU) on day 14 (D14) and day 42 (D42) following *M. tuberculosis* aerosol challenge of naive mice and those receiving SR vaccine or sham vaccine (empty vector). (C) Lung bacillary burden ($\log_{10}$ number of CFU) at day 42 of isoniazid treatment ($n = 4$ animals per data point).

(Fig. 5B). Next, splenocytes from vaccinated mice were collected and stimulated with each recombinant protein (10 μg/ml) for 24 h. DNA vaccination with each poly(P)-regulatory gene generated significant antigen-specific IFN-γ-producing $CD4^+$ T cells compared with vaccination with the vector control (Fig. 5C). Only DNA vaccination with rel_{Mtb} generated significant antigen-specific TNF-α-producing $CD4^+$ T cells compared with vaccination with the vector control.

Immunity engendered by DNA vaccination with poly(P)-regulatory genes enhances the bactericidal activity of isoniazid in mice. To address the potential preventive and therapeutic efficacy of immunity induced by rel_{Mtb}, *sigE*, *ppk2*, and *ppx1*, we combined the four individual DNA plasmids expressing each of these poly(P)-regulatory genes, yielding the stringent response (SR) DNA vaccine. C57BL/6J mice were vaccinated either with the SR vaccine (5 μg of each plasmid) or with the empty vector control (20 μg) once weekly for 4 weeks (Fig. 6A). These mice were aerosol challenged with virulent *M. tuberculosis* strain CDC1551 3 weeks after the last vaccine dose. The lung bacillary burden was not significantly different between vaccinated mice and naive mice at 14 days and 42 days after aerosol challenge (Fig. 6B). A separate

group of mice received human-equivalent doses of isoniazid once daily (5 days/week) by esophageal gavage beginning on day 14 after aerosol challenge (43). Following 28 days of treatment with isoniazid, we observed a significant ($P = 0.013$) reduction in the number of CFU in the lungs of the SR-vaccinated group relative to the number in the lungs of the group receiving the sham vaccine (Fig. 6C). Analysis of lung histology revealed pulmonary inflammation which was commensurate with the lung bacillary burden (see Fig. S2 in the supplemental material). As far as we are aware, this is the first study to show that immunity to poly(P)-regulatory factors of the stringent response pathway enhances the bactericidal activity of the first-line drug isoniazid.

DISCUSSION

The bacterial stringent response appears to play a key role in antibiotic tolerance (2, 44). Poly(P) may serve as a phosphate donor, activating downstream stringent response genes, including *mprAB*, *sigE*, and rel_{Mtb}, thereby leading to antibiotic tolerance in *M. tuberculosis* (7, 9, 10, 15, 45). Previously, we found that the *ppk2*-deficient mutant showed attenuated growth during the acute phase of infection in the murine model but did not show reduced persistence beyond day 56 after infection (15). The *ppx1*-deficient mutant showed a persistence defect in the guinea pig model (9). Similarly, when the *ppk2* gene was disrupted by a mycobacteriophage, the resulting *ppk2*-deficient *M. tuberculosis* strain showed reduced persistence in guinea pigs (11). Our metabolomics analysis revealed that poly(P) accumulation alters the intracellular G3P content in *M. tuberculosis* (Fig. 1). Transcriptional analysis of both mutant strains showed reduced expression of genes involved in G3P synthesis and recycling (Fig. 2). Importantly, G3P can be used as a scaffold for phospholipid biosynthesis (46). Overexpression of glycerol-3-phosphate dehydrogenase in *E. coli* leads to reduced intracellular G3P levels and increased formation of persister cells following exposure to antibiotics (47). G3P and G2P levels are reduced in *M. tuberculosis* when cholesterol is the sole carbon source (48). During chronic *M. tuberculosis* infection of mice, the use of cholesterol is important for bacillary survival (49). Cholesterol accumulation alters *M. tuberculosis* cell wall permeability to rifampin and masks cell wall antigen from binding antibody (50). We have shown previously that a poly(P)-accumulating strain (*ppx2* knockdown) exhibited significant downregulation of the G3P dehydrogenase gene *glpD2* (10), which is also downregulated in *M. tuberculosis* persisters (10, 51). Taken together, these findings suggest that poly(P) serves an important role in downregulating G3P synthesis, which may promote persister formation and antibiotic tolerance (52).

The role of the arginine deiminase pathway during chronic bacterial infections remains controversial. Previous studies have reported the importance of this pathway during microaerobic survival of *Pseudomonas aeruginosa* in the airways of patients with cystic fibrosis (53). L-Arginine deiminase degradation may serve as an alternative carbohydrate utilization pathway during chronic infection in *P. aeruginosa* (54). Infection with *Mycobacterium bovis* BCG leads to enhanced arginine uptake by IFN-γ-stimulated macrophages (55). However, an *M. tuberculosis* strain deficient in the arginine deiminase gene (*arcA*) did not show defective survival during chronic murine infection (31). Our data raise the possibility that poly(P) accumulation leads to upregulation of the arginine deiminase pathway, perhaps reflecting a switch to alternative energy sources. Remodeling of the citric acid cycle, including increased production of succinate and decreased production of α-ketoglutarate, has been observed during *M. tuberculosis* adaptation to hypoxia and following bacillary exposure to antibiotics (56, 57). In *E. coli*, citrate and succinate were found to accumulate during exposure to bactericidal antibiotics (58). In the current study, we found that deficiency of *ppx1* was associated with a significantly increased abundance of succinate and malate. These trends were also observed during *ppk2* deficiency, although they did not achieve statistical significance. Our data suggest that poly(P) accumulation leads to remodeling of the citric acid cycle, although the mechanisms by which these metabolic changes are regulated and how they contribute to antibiotic tolerance remain to be elucidated.

Prior work has focused on the role of poly(P) as a molecular chaperone for stabilizing proteins (59). In the current study, we found accumulation of several amino acid metabolites in the two poly(P)-accumulating strains, particularly in the *ppx1*::Tn mutant. These findings differ from those of a previously reported poly(P)-accumulating strain deficient in *ppx2* (10). This discrepancy may potentially be explained by differences in the function of the two *M. tuberculosis* exopolyphosphatases, PPX1 and PPX2. Specifically, PPX1 hydrolyzes short-chain poly(P) (60), while PPX2 predominantly hydrolyzes long-chain poly(P) (10). The length of individual molecules may dictate the function of poly(P) (59). In addition, these mutant strains were generated using distinct genetic techniques. The previously reported *ppx2*-deficient mutant was generated using a tetracycline-inducible system to overexpress the antisense version of the *ppx2* gene, thereby knocking down its expression, whereas the *ppx1*-deficient mutant used in the current study contains a transposon insertion at bp 732 (total gene length, 1,035 bp), likely disrupting the *ppx1* function. Further studies are needed to elucidate the role of short-chain and long-chain poly(P) in the regulation of individual *M. tuberculosis* metabolic processes.

Poly(P) homeostasis appears to be required for the formation of biofilms. Thus, poly(P) accumulation in *Campylobacter jejuni* (61) and *P. aeruginosa* (62) was associated with defective biofilm formation. Furthermore, deficiency of a polyphosphate kinase responsible for poly(P) synthesis in *P. aeruginosa* also resulted in defective biofilms (63). Null mutants of PPK and PPX in *Bacillus cereus* showed similar defects in biofilm formation (64). Consistent with these findings in other bacteria, we have shown previously (10) and in the current study that maintenance of the intracellular poly(P) balance is required for biofilm formation in *M. tuberculosis*. Interestingly, a recent study found that *ppk2* deficiency did not alter biofilm formation in *M. tuberculosis* (11). Notably, the parental strain used to generate the mutant in our study was CDC1551. This strain has previously been shown to form less biofilm than strain H37Rv (23), which was used by Singh et al. (11). Furthermore, Singh et al. used homologous recombination with temperature-sensitive mycobacteriophages to delete the *ppk2* open reading frame (11), while our study used transposon mutagenesis to disrupt *ppk2*. Relatively little is known about the mechanism by which poly(P) levels modulate biofilm formation. In *E. coli*, poly(P) hydrolysis during stationary phase appears to trigger the formation of biofilms via the LuxS quorum-sensing system (65). Future studies will investigate the role of decreased G3P, remodeling of the citric acid cycle, and altered NADH metabolism on *M. tuberculosis* biofilm formation.

Intracellular accumulation of poly(P) has been linked to *M.*

tuberculosis growth restriction and tolerance to the bactericidal drug isoniazid (9, 15). Our metabolomics analysis revealed alterations in cell wall lipid composition and DXP levels during poly(P) accumulation. By RT-PCR, both mutants showed reduced expression of the L,D-transpeptidase genes, *ldtA* and *ldtB*, which play an important role in peptidoglycan formation of nonreplicating mycobacteria (41). Unlike the *ppx1*-deficient mutant, the *ppk2*-deficient mutant showed increased sensitivity to the L,D-transpeptidase inhibitor meropenem (36), as well as increased expression of *pbpA*. Further studies are required to understand the role of poly(P) accumulation in peptidoglycan synthesis.

The respiration and electron transport pathways are required for the transition of *M. tuberculosis* into persistence and antibiotic tolerance (66, 67). We used the oxidative agent plumbagin to determine if poly(P) accumulation alters sensitivity to inhibitors of respiratory electron transport (38, 68). The *ppk2*::Tn mutant was more sensitive than the wild type and the *ppx1*-deficient mutant to plumbagin, suggesting that *ppk2* deficiency shifts bacteria to a greater dependence on the citric acid cycle and the electron transport chain (69). Furthermore, the *ppx1*-deficient mutant showed increased susceptibility to clofazimine, which destabilizes the bacterial membrane and targets the redox cycling pathway by enzymatic reduction of the drug by NDH-2, the primary respiratory chain NADH:quinone oxidoreductase of mycobacteria, and nonenzymatic oxidation of reduced clofazimine by O_2, yielding reactive oxygen species (39, 70). Future studies will address whether the discrepancies in antibiotic sensitivity between these two poly(P)-accumulating strains result from differences in the enzymatic function of PPX1 and PPK2.

Recently, there has been significant interest in host-directed therapy to treat TB (71). Although BCG vaccination does not enhance the bactericidal activity of chemotherapy in the murine model (72), a DNA vaccine expressing heat shock protein 65 has been shown to synergize with conventional antitubercular drugs, further reducing the bacterial burden in the lungs of *M. tuberculosis*-infected mice or nonhuman primates (72, 73). A fragment whole-cell lysate therapeutic vaccine, RUTI, has shown efficacy in generating protective immunity in preclinical studies (74, 75). However, the primary factors responsible for TB immunity remain unknown. In the current study, we have shown that a DNA vaccine targeting key poly(P)-regulatory factors of the *M. tuberculosis* stringent response generates IgG and antigen-specific $CD4^+$ T cells, but these immune responses did not offer protection against *M. tuberculosis* challenge in the murine model. However, we observed a significant reduction in lung bacillary burden when immunity to these *M. tuberculosis* stringent response factors was combined with isoniazid. One potential explanation for this phenomenon is that the population of persistent bacilli in untreated, chronically infected mice is relatively small (76), but exposure to isoniazid further induces the formation of persisters (77, 78). In favor of this hypothesis, isoniazid exposure induces *M. tuberculosis* expression of rel_{Mtb}, which is required for persister formation (2, 44, 79). Further studies are required to determine the utility of the SR vaccine as a therapeutic vaccine in shortening the duration of treatment in combination with the standard antitubercular regimen or for treating latent *M. tuberculosis* infection.

In summary, poly(P) accumulation appears to induce changes in *M. tuberculosis* metabolism, resulting in altered susceptibility to oxidative stresses and antibiotic exposure and defective biofilm formation. Poly(P) chain length may play an important role in these processes, since we observed several differences between the *ppk2*-deficient and *ppx1*-deficient mutants. Immunity targeting key poly(P)-regulatory factors of the *M. tuberculosis* stringent response augments the tuberculocidal activity of isoniazid in mouse lungs. Future studies will focus on the utility of the stringent response as a potential new target in host-directed therapy for TB.

ACKNOWLEDGMENTS

We have no conflicts of interest to declare.

This work was supported by NIH grants R01HL106786 and UH2AI122309 to P.C.K.

The funding sources had no role in the study design, data collection, data analysis, data interpretation, or writing of the report.

FUNDING INFORMATION

This work, including the efforts of Petros C. Karakousis, was funded by HHS | NIH | National Institute of Allergy and Infectious Diseases (NIAID) (R01HL106786 and UH2AI122309).

REFERENCES

1. **Lawn SD, Zumla AI.** 2011. Tuberculosis. Lancet **378:**57–72. http://dx.doi.org/10.1016/S0140-6736(10)62173-3.
2. **Cohen NR, Lobritz MA, Collins JJ.** 2013. Microbial persistence and the road to drug resistance. Cell Host Microbe **13:**632–642. http://dx.doi.org/10.1016/j.chom.2013.05.009.
3. **Kulaev I, Kulakovskaya T.** 2000. Polyphosphate and phosphate pump. Annu Rev Microbiol **54:**709–734. http://dx.doi.org/10.1146/annurev.micro.54.1.709.
4. **Rao NN, Gomez-Garcia MR, Kornberg A.** 2009. Inorganic polyphosphate: essential for growth and survival. Annu Rev Biochem **78:**605–647. http://dx.doi.org/10.1146/annurev.biochem.77.083007.093039.
5. **Maisonneuve E, Castro-Camargo M, Gerdes K.** 2013. (p)ppGpp controls bacterial persistence by stochastic induction of toxin-antitoxin activity. Cell **154:**1140–1150. http://dx.doi.org/10.1016/j.cell.2013.07.048.
6. **Germain E, Roghanian M, Gerdes K, Maisonneuve E.** 2015. Stochastic induction of persister cells by HipA through (p)ppGpp-mediated activation of mRNA endonucleases. Proc Natl Acad Sci U S A **112:**5171–5176. http://dx.doi.org/10.1073/pnas.1423536112.
7. **Sureka K, Dey S, Datta P, Singh AK, Dasgupta A, Rodrigue S, Basu J, Kundu M.** 2007. Polyphosphate kinase is involved in stress-induced mprAB-sigE-rel signalling in mycobacteria. Mol Microbiol **65:**261–276. http://dx.doi.org/10.1111/j.1365-2958.2007.05814.x.
8. **Sureka K, Sanyal S, Basu J, Kundu M.** 2009. Polyphosphate kinase 2: a modulator of nucleoside diphosphate kinase activity in mycobacteria. Mol Microbiol **74:**1187–1197. http://dx.doi.org/10.1111/j.1365-2958.2009.06925.x.
9. **Thayil SM, Morrison N, Schechter N, Rubin H, Karakousis PC.** 2011. The role of the novel exopolyphosphatase MT0516 in Mycobacterium tuberculosis drug tolerance and persistence. PLoS One **6:**e28076. http://dx.doi.org/10.1371/journal.pone.0028076.
10. **Chuang YM, Bandyopadhyay N, Rifat D, Rubin H, Bader JS, Karakousis PC.** 2015. Deficiency of the novel exopolyphosphatase Rv1026/PPX2 leads to metabolic downshift and altered cell wall permeability in Mycobacterium tuberculosis. mBio **6:**e02428. http://dx.doi.org/10.1128/mBio.02428-14.
11. **Singh M, Tiwari P, Arora G, Agarwal S, Kidwai S, Singh R.** 2016. Establishing virulence associated polyphosphate kinase 2 as a drug target for Mycobacterium tuberculosis. Sci Rep **6:**26900. http://dx.doi.org/10.1038/srep26900.
12. **Shum KT, Lui EL, Wong SC, Yeung P, Sam L, Wang Y, Watt RM, Tanner JA.** 2011. Aptamer-mediated inhibition of Mycobacterium tuberculosis polyphosphate kinase 2. Biochemistry **50:**3261–3271. http://dx.doi.org/10.1021/bi2001455.
13. **Zhu Y, Lee SS, Xu W.** 2003. Crystallization and characterization of polyphosphate kinase from Escherichia coli. Biochem Biophys Res Commun **305:**997–1001. http://dx.doi.org/10.1016/S0006-291X(03)00886-6.
14. **Singh R, Singh M, Arora G, Kumar S, Tiwari P, Kidwai S.** 2013. Polyphosphate deficiency in Mycobacterium tuberculosis is associated with enhanced drug susceptibility and impaired growth in guinea pigs. J Bacteriol **195:**2839–2851. http://dx.doi.org/10.1128/JB.00038-13.

15. **Chuang YM, Belchis DA, Karakousis PC.** 2013. The polyphosphate kinase gene ppk2 is required for Mycobacterium tuberculosis inorganic polyphosphate regulation and virulence. mBio **4:**e00039-13. http://dx.doi.org/10.1128/mBio.00039-13.
16. **Anand A, Verma P, Singh AK, Kaushik S, Pandey R, Shi C, Kaur H, Chawla M, Elechalawar CK, Kumar D, Yang Y, Bhavesh NS, Banerjee R, Dash D, Singh A, Natarajan VT, Ojha AK, Aldrich CC, Gokhale RS.** 2015. Polyketide quinones are alternate intermediate electron carriers during mycobacterial respiration in oxygen-deficient niches. Mol Cell **60:** 637–650. http://dx.doi.org/10.1016/j.molcel.2015.10.016.
17. **Ackart DF, Hascall-Dove L, Caceres SM, Kirk NM, Podell BK, Melander C, Orme IM, Leid JG, Nick JA, Basaraba RJ.** 2014. Expression of antimicrobial drug tolerance by attached communities of Mycobacterium tuberculosis. Pathog Dis **70:**359–369. http://dx.doi.org/10.1111/2049-632X.12144.
18. **Galagan JE, Minch K, Peterson M, Lyubetskaya A, Azizi E, Sweet L, Gomes A, Rustad T, Dolganov G, Glotova I, Abeel T, Mahwinney C, Kennedy AD, Allard R, Brabant W, Krueger A, Jaini S, Honda B, Yu WH, Hickey MJ, Zucker J, Garay C, Weiner B, Sisk P, Stolte C, Winkler JK, Van de Peer Y, Iazzetti P, Camacho D, Dreyfuss J, Liu Y, Dorhoi A, Mollenkopf HJ, Drogaris P, Lamontagne J, Zhou Y, Piquenot J, Park ST, Raman S, Kaufmann SH, Mohney RP, Chelsky D, Moody DB, Sherman DR, Schoolnik GK.** 2013. The Mycobacterium tuberculosis regulatory network and hypoxia. Nature **499:**178–183. http://dx.doi.org/10.1038/nature12337.
19. **Boudonck KJ, Mitchell MW, Nemet L, Keresztes L, Nyska A, Shinar D, Rosenstock M.** 2009. Discovery of metabolomics biomarkers for early detection of nephrotoxicity. Toxicol Pathol **37:**280–292. http://dx.doi.org/10.1177/0192623309332992.
20. **Evans AM, DeHaven CD, Barrett T, Mitchell M, Milgram E.** 2009. Integrated, nontargeted ultrahigh performance liquid chromatography/electrospray ionization tandem mass spectrometry platform for the identification and relative quantification of the small-molecule complement of biological systems. Anal Chem **81:**6656–6667. http://dx.doi.org/10.1021/ac901536h.
21. **Storey JD, Tibshirani R.** 2003. Statistical significance for genomewide studies. Proc Natl Acad Sci U S A **100:**9440–9445. http://dx.doi.org/10.1073/pnas.1530509100.
22. **Zacharia VM, Manzanillo PS, Nair VR, Marciano DK, Kinch LN, Grishin NV, Cox JS, Shiloh MU.** 2013. cor, a novel carbon monoxide resistance gene, is essential for Mycobacterium tuberculosis pathogenesis. mBio **4:**e00721-13. http://dx.doi.org/10.1128/mBio.00721-13.
23. **Pang JM, Layre E, Sweet L, Sherrid A, Moody DB, Ojha A, Sherman DR.** 2012. The polyketide Pks1 contributes to biofilm formation in Mycobacterium tuberculosis. J Bacteriol **194:**715–721. http://dx.doi.org/10.1128/JB.06304-11.
24. **Xu WX, Zhang L, Mai JT, Peng RC, Yang EZ, Peng C, Wang HH.** 2014. The Wag31 protein interacts with AccA3 and coordinates cell wall lipid permeability and lipophilic drug resistance in Mycobacterium smegmatis. Biochem Biophys Res Commun **448:**255–260. http://dx.doi.org/10.1016/j.bbrc.2014.04.116.
25. **Avarbock D, Salem J, Li LS, Wang ZM, Rubin H.** 1999. Cloning and characterization of a bifunctional RelA/SpoT homologue from Mycobacterium tuberculosis. Gene **233:**261–269. http://dx.doi.org/10.1016/S0378-1119(99)00114-6.
26. **Sun Y, Peng S, Qiu J, Miao J, Yang B, Jeang J, Hung CF, Wu TC.** 2015. Intravaginal HPV DNA vaccination with electroporation induces local $CD8^+$ T-cell immune responses and antitumor effects against cervicovaginal tumors. Gene Ther **22:**528–535. http://dx.doi.org/10.1038/gt.2015.17.
27. **Peng S, Song L, Knoff J, Wang JW, Chang YN, Hannaman D, Wu TC, Alvarez RD, Roden RB, Hung CF.** 2014. Control of HPV-associated tumors by innovative therapeutic HPV DNA vaccine in the absence of $CD4^+$ T cells. Cell Biosci **4:**11. http://dx.doi.org/10.1186/2045-3701-4-11.
28. **Cheng WF, Hung CF, Hsu KF, Chai CY, He L, Ling M, Slater LA, Roden RB, Wu TC.** 2001. Enhancement of Sindbis virus self-replicating RNA vaccine potency by targeting antigen to endosomal/lysosomal compartments. Hum Gene Ther **12:**235–252. http://dx.doi.org/10.1089/10430340150218387.
29. **Dutta NK, Illei PB, Jain SK, Karakousis PC.** 2014. Characterization of a novel necrotic granuloma model of latent tuberculosis infection and reactivation in mice. Am J Pathol **184:**2045–2055. http://dx.doi.org/10.1016/j.ajpath.2014.03.008.
30. **Heuston S, Begley M, Gahan CG, Hill C.** 2012. Isoprenoid biosynthesis in bacterial pathogens. Microbiology **158:**1389–1401. http://dx.doi.org/10.1099/mic.0.051599-0.
31. **Surken M, Keller C, Rohker C, Ehlers S, Bange FC.** 2008. Anaerobic arginine metabolism of Mycobacterium tuberculosis is mediated by arginine deiminase (arcA), but is not essential for chronic persistence in an aerogenic mouse model of infection. Int J Med Microbiol **298:**657–661. http://dx.doi.org/10.1016/j.ijmm.2007.09.003.
32. **Cole ST, Brosch R, Parkhill J, Garnier T, Churcher C, Harris D, Gordon SV, Eiglmeier K, Gas S, Barry CE, III, Tekaia F, Badcock K, Basham D, Brown D, Chillingworth T, Connor R, Davies R, Devlin K, Feltwell T, Gentles S, Hamlin N, Holroyd S, Hornsby T, Jagels K, Krogh A, McLean J, Moule S, Murphy L, Oliver K, Osborne J, Quail MA, Rajandream MA, Rogers J, Rutter S, Seeger K, Skelton J, Squares R, Squares S, Sulston JE, Taylor K, Whitehead S, Barrell BG.** 1998. Deciphering the biology of Mycobacterium tuberculosis from the complete genome sequence. Nature **393:**537–544. http://dx.doi.org/10.1038/31159.
33. **Deng X, Weerapana E, Ulanovskaya O, Sun F, Liang H, Ji Q, Ye Y, Fu Y, Zhou L, Li J, Zhang H, Wang C, Alvarez S, Hicks LM, Lan L, Wu M, Cravatt BF, He C.** 2013. Proteome-wide quantification and characterization of oxidation-sensitive cysteines in pathogenic bacteria. Cell Host Microbe **13:**358–370. http://dx.doi.org/10.1016/j.chom.2013.02.004.
34. **Ladjouzi R, Bizzini A, van Schaik W, Zhang X, Rince A, Benachour A, Hartke A.** 2015. Loss of antibiotic tolerance in Sod-deficient mutants is dependent on the energy source and arginine catabolism in enterococci. J Bacteriol **197:**3283–3293. http://dx.doi.org/10.1128/JB.00389-15.
35. **Larrouy-Maumus G, Biswas T, Hunt DM, Kelly G, Tsodikov OV, de Carvalho LP.** 2013. Discovery of a glycerol 3-phosphate phosphatase reveals glycerophospholipid polar head recycling in Mycobacterium tuberculosis. Proc Natl Acad Sci U S A **110:**11320–11325. http://dx.doi.org/10.1073/pnas.1221597110.
36. **Kumar P, Arora K, Lloyd JR, Lee IY, Nair V, Fischer E, Boshoff HI, Barry CE, III.** 2012. Meropenem inhibits D,D-carboxypeptidase activity in Mycobacterium tuberculosis. Mol Microbiol **86:**367–381. http://dx.doi.org/10.1111/j.1365-2958.2012.08199.x.
37. **Lavollay M, Arthur M, Fourgeaud M, Dubost L, Marie A, Veziris N, Blanot D, Gutmann L, Mainardi JL.** 2008. The peptidoglycan of stationary-phase Mycobacterium tuberculosis predominantly contains cross-links generated by L,D-transpeptidation. J Bacteriol **190:**4360–4366. http://dx.doi.org/10.1128/JB.00239-08.
38. **Hasan MR, Rahman M, Jaques S, Purwantini E, Daniels L.** 2010. Glucose 6-phosphate accumulation in mycobacteria: implications for a novel F420-dependent anti-oxidant defense system. J Biol Chem **285:** 19135–19144. http://dx.doi.org/10.1074/jbc.M109.074310.
39. **Cholo MC, Steel HC, Fourie PB, Germishuizen WA, Anderson R.** 2012. Clofazimine: current status and future prospects. J Antimicrob Chemother **67:**290–298. http://dx.doi.org/10.1093/jac/dkr444.
40. **Pavelka MS, Jr, Mahapatra S, Crick DC.** 2014. Genetics of peptidoglycan biosynthesis. Microbiol Spectr **2:**MGM2-0034-2013. http://dx.doi.org/10.1128/microbiolspec.MGM2-0034-2013.
41. **Dubee V, Triboulet S, Mainardi JL, Etheve-Quelquejeu M, Gutmann L, Marie A, Dubost L, Hugonnet JE, Arthur M.** 2012. Inactivation of Mycobacterium tuberculosis L,D-transpeptidase LdtMt(1) by carbapenems and cephalosporins. Antimicrob Agents Chemother **56:**4189–4195. http://dx.doi.org/10.1128/AAC.00665-12.
42. **Adams KN, Szumowski JD, Ramakrishnan L.** 2014. Verapamil, and its metabolite norverapamil, inhibit macrophage-induced, bacterial efflux pump-mediated tolerance to multiple anti-tubercular drugs. J Infect Dis **210:**456–466. http://dx.doi.org/10.1093/infdis/jiu095.
43. **Dutta NK, Pinn ML, Karakousis PC.** 2014. Reduced emergence of isoniazid resistance with concurrent use of thioridazine against acute murine tuberculosis. Antimicrob Agents Chemother **58:**4048–4053. http://dx.doi.org/10.1128/AAC.02981-14.
44. **Boutte CC, Crosson S.** 2013. Bacterial lifestyle shapes stringent response activation. Trends Microbiol **21:**174–180. http://dx.doi.org/10.1016/j.tim.2013.01.002.
45. **Sanyal S, Banerjee SK, Banerjee R, Mukhopadhyay J, Kundu M.** 2013. Polyphosphate kinase 1, a central node in the stress response network of Mycobacterium tuberculosis, connects the two-component systems MprAB and SenX3-RegX3 and the extracytoplasmic function sigma factor, sigma E. Microbiology **159:**2074–2086. http://dx.doi.org/10.1099/mic.0.068452-0.
46. **Kanehisa M, Goto S, Hattori M, Aoki-Kinoshita KF, Itoh M, Ka-**

washima S, Katayama T, Araki M, Hirakawa M. 2006. From genomics to chemical genomics: new developments in KEGG. Nucleic Acids Res **34:** D354–D357. http://dx.doi.org/10.1093/nar/gkj102.
47. **Spoering AL, Vulic M, Lewis K.** 2006. GlpD and PlsB participate in persister cell formation in Escherichia coli. J Bacteriol **188:**5136–5144. http://dx.doi.org/10.1128/JB.00369-06.
48. **Griffin JE, Pandey AK, Gilmore SA, Mizrahi V, McKinney JD, Bertozzi CR, Sassetti CM.** 2012. Cholesterol catabolism by Mycobacterium tuberculosis requires transcriptional and metabolic adaptations. Chem Biol **19:** 218–227. http://dx.doi.org/10.1016/j.chembiol.2011.12.016.
49. **Pandey AK, Sassetti CM.** 2008. Mycobacterial persistence requires the utilization of host cholesterol. Proc Natl Acad Sci U S A **105:**4376–4380. http://dx.doi.org/10.1073/pnas.0711159105.
50. **Brzostek A, Pawelczyk J, Rumijowska-Galewicz A, Dziadek B, Dziadek J.** 2009. Mycobacterium tuberculosis is able to accumulate and utilize cholesterol. J Bacteriol **191:**6584–6591. http://dx.doi.org/10.1128/JB.00488-09.
51. **Keren I, Minami S, Rubin E, Lewis K.** 2011. Characterization and transcriptome analysis of Mycobacterium tuberculosis persisters. mBio **2:**e00100-11. http://dx.doi.org/10.1128/mBio.00100-11.
52. **Lewis K.** 2007. Persister cells, dormancy and infectious disease. Nat Rev Microbiol **5:**48–56. http://dx.doi.org/10.1038/nrmicro1557.
53. **Hogardt M, Heesemann J.** 2010. Adaptation of Pseudomonas aeruginosa during persistence in the cystic fibrosis lung. Int J Med Microbiol **300:**557–562. http://dx.doi.org/10.1016/j.ijmm.2010.08.008.
54. **Palmer KL, Aye LM, Whiteley M.** 2007. Nutritional cues control Pseudomonas aeruginosa multicellular behavior in cystic fibrosis sputum. J Bacteriol **189:**8079–8087. http://dx.doi.org/10.1128/JB.01138-07.
55. **Peteroy-Kelly M, Venketaraman V, Connell ND.** 2001. Effects of Mycobacterium bovis BCG infection on regulation of L-arginine uptake and synthesis of reactive nitrogen intermediates in J774.1 murine macrophages. Infect Immun **69:**5823–5831. http://dx.doi.org/10.1128/IAI.69.9.5823-5831.2001.
56. **Eoh H, Rhee KY.** 2013. Multifunctional essentiality of succinate metabolism in adaptation to hypoxia in Mycobacterium tuberculosis. Proc Natl Acad Sci U S A **110:**6554–6559. http://dx.doi.org/10.1073/pnas.1219375110.
57. **Nandakumar M, Nathan C, Rhee KY.** 2014. Isocitrate lyase mediates broad antibiotic tolerance in Mycobacterium tuberculosis. Nat Commun **5:**4306. http://dx.doi.org/10.1038/ncomms5306.
58. **Belenky P, Ye JD, Porter CB, Cohen NR, Lobritz MA, Ferrante T, Jain S, Korry BJ, Schwarz EG, Walker GC, Collins JJ.** 2015. Bactericidal antibiotics induce toxic metabolic perturbations that lead to cellular damage. Cell Rep **13:**968–980. http://dx.doi.org/10.1016/j.celrep.2015.09.059.
59. **Gray MJ, Wholey WY, Wagner NO, Cremers CM, Mueller-Schickert A, Hock NT, Krieger AG, Smith EM, Bender RA, Bardwell JC, Jakob U.** 2014. Polyphosphate is a primordial chaperone. Mol Cell **53:**689–699. http://dx.doi.org/10.1016/j.molcel.2014.01.012.
60. **Choi MY, Wang Y, Wong LL, Lu BT, Chen WY, Huang JD, Tanner JA, Watt RM.** 2012. The two PPX-GppA homologues from Mycobacterium tuberculosis have distinct biochemical activities. PLoS One **7:**e42561. http://dx.doi.org/10.1371/journal.pone.0042561.
61. **Malde A, Gangaiah D, Chandrashekhar K, Pina-Mimbela R, Torrelles JB, Rajashekara G.** 2014. Functional characterization of exopolyphosphatase/guanosine pentaphosphate phosphohydrolase (PPX/GPPA) of Campylobacter jejuni. Virulence **5:**521–533. http://dx.doi.org/10.4161/viru.28311.
62. **Gallarato LA, Sanchez DG, Olvera L, Primo ED, Garrido MN, Beassoni PR, Morett E, Lisa AT.** 2014. Exopolyphosphatase of Pseudomonas aeruginosa is essential for the production of virulence factors, and its expression is controlled by NtrC and PhoB acting at two interspaced promoters. Microbiology **160:**406–417. http://dx.doi.org/10.1099/mic.0.074773-0.
63. **Fraley CD, Rashid MH, Lee SS, Gottschalk R, Harrison J, Wood PJ, Brown MR, Kornberg A.** 2007. A polyphosphate kinase 1 (ppk1) mutant of Pseudomonas aeruginosa exhibits multiple ultrastructural and functional defects. Proc Natl Acad Sci U S A **104:**3526–3531. http://dx.doi.org/10.1073/pnas.0609733104.
64. **Shi X, Rao NN, Kornberg A.** 2004. Inorganic polyphosphate in Bacillus cereus: motility, biofilm formation, and sporulation. Proc Natl Acad Sci U S A **101:**17061–17065. http://dx.doi.org/10.1073/pnas.0407787101.
65. **Grillo-Puertas M, Villegas JM, Rintoul MR, Rapisarda VA.** 2012. Polyphosphate degradation in stationary phase triggers biofilm formation via LuxS quorum sensing system in Escherichia coli. PLoS One **7:**e50368. http://dx.doi.org/10.1371/journal.pone.0050368.
66. **Baek SH, Li AH, Sassetti CM.** 2011. Metabolic regulation of mycobacterial growth and antibiotic sensitivity. PLoS Biol **9:**e1001065. http://dx.doi.org/10.1371/journal.pbio.1001065.
67. **Black PA, Warren RM, Louw GE, van Helden PD, Victor TC, Kana BD.** 2014. Energy metabolism and drug efflux in Mycobacterium tuberculosis. Antimicrob Agents Chemother **58:**2491–2503. http://dx.doi.org/10.1128/AAC.02293-13.
68. **Mathew R, Kruthiventi AK, Prasad JV, Kumar SP, Srinu G, Chatterji D.** 2010. Inhibition of mycobacterial growth by plumbagin derivatives. Chem Biol Drug Des **76:**34–42. http://dx.doi.org/10.1111/j.1747-0285.2010.00987.x.
69. **Reddy PJ, Ray S, Sathe GJ, Prasad TS, Rapole S, Panda D, Srivastava S.** 2015. Proteomics analyses of Bacillus subtilis after treatment with plumbagin, a plant-derived naphthoquinone. OMICS **19:**12–23. http://dx.doi.org/10.1089/omi.2014.0099.
70. **Yano T, Kassovska-Bratinova S, Teh JS, Winkler J, Sullivan K, Isaacs A, Schechter NM, Rubin H.** 2011. Reduction of clofazimine by mycobacterial type 2 NADH:quinone oxidoreductase: a pathway for the generation of bactericidal levels of reactive oxygen species. J Biol Chem **286:**10276–10287. http://dx.doi.org/10.1074/jbc.M110.200501.
71. **Wallis RS, Hafner R.** 2015. Advancing host-directed therapy for tuberculosis. Nat Rev Immunol **15:**255–263. http://dx.doi.org/10.1038/nri3813.
72. **Silva CL, Bonato VL, Coelho-Castelo AA, De Souza AO, Santos SA, Lima KM, Faccioli LH, Rodrigues JM.** 2005. Immunotherapy with plasmid DNA encoding mycobacterial hsp65 in association with chemotherapy is a more rapid and efficient form of treatment for tuberculosis in mice. Gene Ther **12:**281–287. http://dx.doi.org/10.1038/sj.gt.3302418.
73. **Kita Y, Hashimoto S, Nakajima T, Nakatani H, Nishimatsu S, Nishida Y, Kanamaru N, Kaneda Y, Takamori Y, McMurray D, Tan EV, Cang ML, Saunderson P, Dela Cruz EC, Okada M.** 2013. Novel therapeutic vaccines [(HSP65 + IL-12)DNA-, granulysin- and Ksp37-vaccine] against tuberculosis and synergistic effects in the combination with chemotherapy. Hum Vaccin Immunother **9:**526–533. http://dx.doi.org/10.4161/hv.23230.
74. **Nell AS, D'Lom E, Bouic P, Sabate M, Bosser R, Picas J, Amat M, Churchyard G, Cardona PJ.** 2014. Safety, tolerability, and immunogenicity of the novel antituberculous vaccine RUTI: randomized, placebo-controlled phase II clinical trial in patients with latent tuberculosis infection. PLoS One **9:**e89612. http://dx.doi.org/10.1371/journal.pone.0089612.
75. **Cardona PJ.** 2006. RUTI: a new chance to shorten the treatment of latent tuberculosis infection. Tuberculosis (Edinb) **86:**273–289. http://dx.doi.org/10.1016/j.tube.2006.01.024.
76. **Gill WP, Harik NS, Whiddon MR, Liao RP, Mittler JE, Sherman DR.** 2009. A replication clock for Mycobacterium tuberculosis. Nat Med **15:** 211–214. http://dx.doi.org/10.1038/nm.1915.
77. **Ahmad Z, Klinkenberg LG, Pinn ML, Fraig MM, Peloquin CA, Bishai WR, Nuermberger EL, Grosset JH, Karakousis PC.** 2009. Biphasic kill curve of isoniazid reveals the presence of drug-tolerant, not drug-resistant, Mycobacterium tuberculosis in the guinea pig. J Infect Dis **200:** 1136–1143. http://dx.doi.org/10.1086/605605.
78. **Karakousis PC, Williams EP, Bishai WR.** 2008. Altered expression of isoniazid-regulated genes in drug-treated dormant Mycobacterium tuberculosis. J Antimicrob Chemother **61:**323–331.
79. **Boshoff HI, Myers TG, Copp BR, McNeil MR, Wilson MA, Barry CE, III.** 2004. The transcriptional responses of Mycobacterium tuberculosis to inhibitors of metabolism: novel insights into drug mechanisms of action. J Biol Chem **279:**40174–40184. http://dx.doi.org/10.1074/jbc.M406796200.